

Characteristics of magnetospheric energetics during geomagnetic storms

H. Li,^{1,2} C. Wang,¹ W. Y. Xu,³ and J. R. Kan^{1,4}

Received 31 January 2012; revised 12 March 2012; accepted 14 March 2012; published 28 April 2012.

[1] To investigate the magnetospheric energetics during magnetic storms, we performed a statistical survey of 307 geomagnetic storms between 1995 and 2009. For the purpose of getting a detailed understanding of the energy processes, we conducted our study of storm-time energetics for three time durations: the main phase, the recovery phase, and the total storm period. We found that the partition of the energy dissipation via the ring current injection and high-latitude ionospheric dissipation is controlled by the storm intensity. The proportion of the ring current injection increases linearly as the storm intensity increases for all three time durations. For moderate storms, the high-latitude ionospheric dissipation is dominant, with only $\sim 30\%$ energy dissipated via the ring current; whereas for superstorms, the ring current injection becomes dominant, with $\sim 70\%$ energy dissipated via the ring current. We also confirmed the essential and crucial role of the total energy input into the magnetosphere during the main phase in controlling the storm intensity. The total energy input during the main phase is directly proportional to the storm intensity. Their correlation efficiency is as high as 0.85. The storm-time energy budget was also quantified in this study. The coupling efficiency indicates an exponential decay as the storm intensity increases, with the coupling efficiency during the main phase less than that during the recovery phase.

Citation: Li, H., C. Wang, W. Y. Xu, and J. R. Kan (2012), Characteristics of magnetospheric energetics during geomagnetic storms, *J. Geophys. Res.*, *117*, A04225, doi:10.1029/2012JA017584.

1. Introduction

[2] The study of energy transmission, conversion, and dissipation in the solar wind-magnetosphere-ionosphere (SW-M-I) coupling system during geomagnetic storms is a fundamental issue in Solar-Terrestrial Physics. The research of energy coupling process in the SW-M-I coupling system began in early 1960s. To understand and to quantify how the energy is carried and transferred by the solar wind, and how it is converted and dissipated in the magnetosphere-ionosphere (M-I) system, especially during magnetic storms, has been recognized as important steps to understand the near-Earth environment and for space weather prediction.

[3] Magnetosphere can be regarded as an enormous reservoir, which stores the energy transported from the solar wind. Most of the energy input into the magnetosphere has been understood to be a consequence of the dayside

magnetic reconnection [Dungey, 1961]. The orientation of the interplanetary magnetic field (IMF) plays a dominant role in the energy transfer [e.g., Burton *et al.*, 1975; Akasofu, 1981]. More energy would be transported into the magnetosphere during the southward IMF than the northward IMF. When the interplanetary disturbance has a long-duration and intense southward IMF [Tsurutani and Gonzalez, 1997], the magnetosphere will become very active, resulting in a geomagnetic storm. Subsequently, the previously stored energy in the magnetosphere apportioned amongst various “branches” in the M-I coupling system. The two major “branches” are: the ring current injection and the high-latitude ionospheric energy dissipation [Akasofu, 1981; Weiss *et al.*, 1992; Baker *et al.*, 1997; Knipp *et al.*, 1998].

[4] The study about the storm-time energetics of the SW-M-I coupling system can be divided into three aspects: (1) the energy input into the magnetosphere from the solar wind and its input efficiency, (2) the partition of the energy dissipation in the inner M-I system, (3) the energy budget during magnetic storms. Many studies about the storm-time magnetospheric energetics have been done in the last several decades. Most of the studies were case analysis based on data for less than 10 magnetic storms [Perreault and Akasofu, 1978; Gonzalez *et al.*, 1989; Mac-Mahon and Gonzalez, 1997; Lu *et al.*, 1998; Turner, 2000; Baker *et al.*, 2001; Feldstein *et al.*, 2003; Vichare *et al.*, 2005; Rosenqvist *et al.*, 2006]. Some found that the ring current injection was dominant in the partition of energy dissipation in the inner M-I system, by analyzing 4 to 9 extreme intense storms (the mean

¹State Key Laboratory of Space Weather, National Space Science Center, Chinese Academy of Sciences, Beijing, China.

²Key Laboratory of Geospace Environment, University of Science and Technology of China, Chinese Academy of Sciences, Hefei, China.

³Institute of Geology and Geophysics, Chinese Academy of Sciences, Beijing, China.

⁴Geophysical Institute, University of Alaska Fairbanks, Alaska, USA.

Corresponding Author: H. Li, State Key Laboratory of Space Weather, National Space Science Center, Chinese Academy of Sciences, Beijing, China. (hli@spaceweather.ac.cn)

Dst index was ~ -260 nT, for their cases) [e.g., *Mac-Mahon and Gonzalez*, 1997; *Vichare et al.*, 2005]; others argued that the ionospheric dissipation was dominant in the partition of energy dissipation, based on the analysis of several moderate to intense storms (the mean *Dst* was ~ -127 nT, for their cases) [e.g., *Lu et al.*, 1998; *Knipp et al.*, 1998; *Baker et al.*, 2001; *Feldstein et al.*, 2003].

[5] Besides many case analysis, there are few statistical studies about the storm-time energy coupling processes, which mainly paid attention to the discrepancies due to different interplanetary driving structures, such as corotating interaction regions (CIRs), coronal mass ejections (CMEs), and sheath regions. *Turner et al.* [2009] found that the ratio of energy dissipation to energy input for the CIR-driven storms was greater than that for CME-driven storms. *Guo et al.* [2011] also argued the differences in the energy transfer between the sheath-driven storms and CME-driven storms. These kinds of differing approaches likely have influenced the energy coupling processes for each storm. It is very difficult for case analysis to take that into consideration. Meanwhile, the differences among storm events make it hard to reflect a universal law for case analysis. Therefore, a detailed statistical survey of the relationship between the storm-time energetics and storm intensity is still of interests.

[6] In this work, we performed a statistical survey of 307 magnetic storms with $SYMH \leq -50$ nT for the period between 1995 and 2009, which covers more than an entire solar cycle. Among the 307 storms, there are 213 moderate storms ($-100 < SYMH \leq -50$ nT), 88 intense storms ($-300 < SYMH \leq -100$ nT) and 6 superstorms ($SYMH \leq -300$ nT, suggested by *Li et al.* [2010]). The 307 storms cover all possible driving structures. This would give a comprehensive view of storm-time magnetospheric energetics. The energetics involved in the storm main phase, the recovery phase and the total storm period, are investigated separately to gain a detailed understanding of the energy processes. The energetics of the solar wind and the inner M-I coupling system are presented in section 2. The statistical results are shown in section 3. Section 4 and section 5 give the discussion and concluding remarks, respectively.

2. Energetics of the Solar Wind and M-I System

[7] To accurately monitor the energy transportation from the solar wind and energy dissipation in the inner magnetosphere is almost impossible at the present stage. Some empirical formulas have to be proposed and used to make the rough estimations.

2.1. Energetics of the Solar Wind

[8] The kinetic energy of the solar wind impinging on the dayside magnetopause per unit time can be estimated as

$$U_{SW} = \frac{1}{2} \cdot \rho \cdot V_{SW}^3 \cdot A \quad (1)$$

where ρ and V_{SW} are the mass density and bulk velocity of the solar wind, respectively, and A is the cross section of the dayside magnetopause and is suggested to be $(30 R_E)^2$ [*Weiss et al.*, 1992]. *Mac-Mahon and Gonzalez* [1997] argued that $(30 R_E)^2$ was an overestimation, and the variation of the dayside magnetopause boundary due to varying

nature of the solar wind dynamic pressure should be considered. Therefore in practice, we use the cross section along the dawn-dusk meridian of the magnetopause suggested by *Lu et al.* [1998] instead of $(30 R_E)^2$ in this study, which is given by $A = \pi \times (r_0 \cdot 2^\alpha)^2$. r_0 and α , representing the standoff distance at the subsolar point and the level of tail flaring, can be obtained from *Shue-98* magnetopause model [*Shue et al.* 1998].

[9] Although there has not been an accurate measurement of the total energy input from the solar wind into the magnetosphere at any given time, we can still use the accepted existing parameters to estimate this quantity. Several SW-M-I coupling parameters have been proposed over the years [*Nishida*, 1983; *Newell et al.*, 2007, and references therein]. The most widely used coupling parameter given by *Perreault and Akasofu* [1978] in the SI units is as

$$U_\varepsilon = \frac{4\pi}{\mu_0} V_{SW} B_{SW}^2 \sin^4\left(\frac{\theta_c}{2}\right) l_0^2 \quad (2)$$

where μ_0 is the magnetic permeability of free space, B_{SW} is the magnitude of the interplanetary magnetic field (IMF), θ_c is the IMF clock angle, and l_0 denotes the linear dimension of the “effective cross-sectional area” of the solar wind-magnetosphere interaction and was determined empirically to be $7 R_E$ [*Perreault and Akasofu*, 1978]. From equation (2) we can see that U_ε maximizes when IMF turns southward, and even under weak northward IMF conditions, significant energy coupling is still possible. The U_ε parameter has been proven to be a very useful tool in energy analysis. Many studies have shown that the coupling parameter gives a reasonable estimate of the total energy transferred into the magnetosphere [e.g., *Zwickl et al.*, 1987; *Baker et al.*, 1997; *Lu et al.*, 1998; *Liou et al.*, 1998].

[10] However, *Koskinen and Tanskanen* [2002] suggested that a scaling parameter of 1.5–2 should be applied to the coupling parameters to account for some substorm-related tail energy sinks, such as escape energy carried by plasmoids and plasma sheet heating. By considering the variation of subsolar point of dayside magnetopause, *Mac-Mahon and Gonzalez* [1997] and *Vichare et al.* [2005] used the Chapman-Ferraro magnetopause distance (L_{CF}) instead of $7 R_E$, which can be obtained from the balance between the kinetic plasma pressure and the geomagnetic pressure [e.g., *Sibeck et al.*, 1991],

$$L_{CF} = (B_0^2 / 4\pi\rho V_{SW}^2)^{1/6} (R_E) \quad (3)$$

where B_0 is the Earth’s magnetic field strength, ~ 0.3 Gauss. For comparison, these three different l_0 values: $7 R_E$, L_{CF} and r_0 , would all be used to estimate the total energy input into the magnetosphere as presented in section 3.

2.2. Ring Current Injection Rate

[11] For many years, the hourly *Dst* index has been used to estimate the total ring current energy content during magnetic storms. Besides the ring current, other magnetospheric current systems can also contribute to the *Dst* index, such as the dayside magnetopause current, the cross-tail current, and the ground-induced currents (see *Maltsev* [2004] for details). Therefore, additional adjustments to the measured *Dst* index are needed in estimating the ring current injection. *Burton*

Table 1. Six Typical Models of the Ring Current Decay Time (τ)

Model	Decay Time τ (h)	Reference
BM1975	7.7	Burton <i>et al.</i> [1975]
A1981	20 for $\varepsilon < 100$ GW 6 for $100 < \varepsilon \leq 500$ GW 3 for $500 < \varepsilon \leq 1000$ GW 1 for $1000 < \varepsilon \leq 5000$ GW 0.3 for $5000 < \varepsilon \leq 10000$ GW 0.2 for $\varepsilon > 10000$ GW $\varepsilon = U_{\infty}, l_0 = 7R_E$	Akasofu [1981]
G1993	4 for $Dst \geq -50$ nT 2 for $-50 > Dst \geq -100$ nT 1 for $-100 > Dst \geq -200$ nT 0.5 for $-200 > Dst \geq -300$ nT 0.25 for $Dst < -300$ nT	Gonzalez [1993]
VS1996	12.5/(1.0 - 0.0012 <i>Dst</i>)	Valdivia <i>et al.</i> [1996]
OM2000	2.40exp[9.74/(4.69 + <i>VB_S</i>)]	O'Brien and McPherron [2000]
XD2010	1/(0.1 + 3.0 × 10 ⁻⁴ ε[GW])	Xu and Du [2010]

et al. [1975] proposed the following formula to remove the magnetopause current contribution from the measured *Dst*.

$$Dst^* = Dst - b\sqrt{P_d} + c \quad (4)$$

where *Dst** is the pressure-corrected *Dst* index, *P_d* is the solar wind dynamic pressure. Various values for the coefficients *b* and *c* have been proposed according to different models [e.g., Gonzalez *et al.*, 1994; O'Brien and McPherron, 2000; Turner *et al.*, 2001]. The differences of the coefficients *b* and *c* for different models are not significant. In practice, we choose *b* = 7.26 (nT · nPa^{-1/2}) and *c* = 11.0 (nT) [O'Brien and McPherron, 2000] here. Furthermore, Turner *et al.* [2001] argued that the contributions of the ground-induced current and the cross-tail currents account for about 21% and 25% of the *Dst**, respectively. Hence, *Dst** should be scaled down to 54% (*Dst****) to only reflect the ring current contribution.

[12] After these adjustments to the *Dst* index, the rate of energy injection (*U_{RC}*) into the ring current particle population was then calculated using the relationship derived by Akasofu [1981]. The formula in SI units is as

$$U_{RC}(GW) = -4 \times 10^4 \left(\frac{\partial Dst^{**}}{\partial t} - \frac{Dst^{**}}{\tau} \right) \quad (5)$$

where *Dst*** is expressed in nT and τ is the ring current decay time given in seconds. The ring current lifetime (τ) plays a important and sensitive role in estimating the magnitude of ring current injection. Many discussions on the ring current lifetime have been proposed in the literature (see Feldstein [1992] for a review) [Prigancova and Feldstein, 1992; Gonzalez, 1993; Valdivia *et al.*, 1996; Mac-Mahon and Gonzalez, 1997; Lu *et al.*, 1998; O'Brien and McPherron, 2000; Xu and Du, 2010]. Table 1 lists six typical models of the ring current decay rate. And we would estimate the ring current injection by using all these six models for comparison.

[13] The *SYM*H index is essentially the same as the hourly *Dst* index with a higher time resolution of 1 min. We would use the *SYM*H index instead of the *Dst* index in the following calculations.

2.3. Ionospheric Dissipation Rate

[14] The ionospheric energy dissipation in the form of Joule heating and particle precipitation can be determined locally from the data collected by, e.g., rocket-born instruments or the incoherent scatter radar. However, there is still a challenge to monitor the two energy processes on a global scale accurately. Several empirical relations have been developed [e.g., Akasofu, 1981; Ahn *et al.*, 1983, 1989; Baumjohann and Kamide, 1984; Richmond *et al.*, 1990; Cooper *et al.*, 1995; Lu *et al.*, 1995, 1998; Østgaard *et al.*, 2002a, 2002b; Knipp *et al.*, 2004]. Most of them used the *AE* or *AL* index to do the estimation.

[15] Akasofu [1981] used the *AE* index as the first approximation measurements of the global Joule heating rate (*U_J*) and auroral particle precipitation (*U_A*). Further studies showed that the Joule heating dissipation has a seasonal dependence. The summer hemisphere accounts for about 60% of the total Joule heating dissipation, while the winter hemisphere only dissipation about 40% [Østgaard *et al.*, 2002a]. Empirical relations that account for this summer and winter asymmetry are summarized by Østgaard *et al.* [2002a, 2002b] as follows:

$$U_J(GW) = 0.54 \times AE + 1.8 \quad (6)$$

$$U_A(GW) = 2 \times (4.4\sqrt{AL} - 7.6) \quad (7)$$

We would use these two empirical formulas to estimate the global Joule heating and auroral particle precipitation.

3. Statistical Results

[16] In our analysis, 307 magnetic storms with *SYM*H ≤ -50 nT are analyzed for the period between 1995 and 2009, which covers more than an entire solar cycle. The minimum *SYM*H index is defined as the storm intensity. By using the 5-min solar wind data from OMNI group and the 5-min averaged *SYM*H, *AE* and *AL* index, we estimate the rate of kinetic energy of the solar wind, the energy input, the ring current injection, the Joule heating and the auroral particle precipitation for each storm from equation (1), (2), (5), (6) and (7), respectively. For the purpose of getting a detailed understanding of the energy processes, all parts of the total energy involved in the storm main phase, the recovery phase and the total storm period were obtained separately by integrating the rates of energy processes over the corresponding time intervals. For each storm, we determined four time points to do the time integration, the start time of the sudden or slowly increase of the *SYM*H index (*t*₁), the start time of sudden decrease of the *SYM*H index (*t*₂), the time when the *SYM*H index reached its minimum (*t*₃), and the time when the *SYM*H index first recovered to four fifths of its minimum during the recovery phase (*t*₄). The main phase was defined as the time interval between *t*₂ and *t*₃; the recovery phase *t*₂ was defined as the time interval between *t*₃ and *t*₄; the total storm was defined as the time interval between *t*₁ and *t*₄. The statistical results are presented in the following subsections.

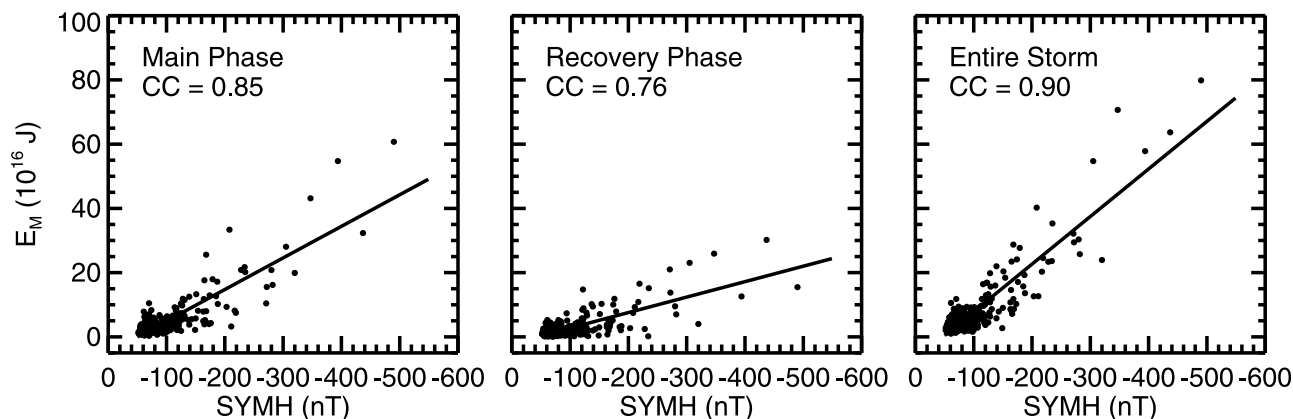


Figure 1. The relationship between the total energy input (E_M) and the storm intensity. The results for the durations of the main phase, the recovery phase and the total storm period are shown successively from left to right. CC is the correlation coefficient.

3.1. Energy Input and Its Efficiency

[17] The total solar wind kinetic energy (E_{SW}) and the total energy transported into the magnetosphere (E_M) are calculated in the units of Joules, by integrating the corresponding energy flux rates shown in equation (1) and (2) over the time, respectively. A parameter $IE = E_M/E_{SW} \times 100\%$ is also used to study the input efficiency of energy enters from the solar wind into the magnetosphere.

[18] So far, a large number of studies about the relationship between the solar wind conditions and the corresponding storm intensity have been performed in the literature. Compared to the solar wind parameters, the total energy input into the magnetosphere during the main phase of a storm should play a more essential and crucial role in controlling the storm intensity. Figure 1 shows the relationship between the total energy input, E_M , and the storm intensity. In practice, we chose $l_0 = 7R_E$ when calculating U_ϵ . The E_M during the main phase, the recovery phase and the total storm period varies widely from 0.3×10^{16} J to 60.7×10^{16} J, from 0.05×10^{16} J to 30.2×10^{16} J, and from 1.0×10^{16} J to 79.9×10^{16} J, respectively. However, the total energy input E_M is highly correlated with the storm intensity. The linear correlation coefficient for the main phase, the recovery phase and the total storm period is as high as 0.85, 0.76 and 0.90, respectively. These characteristics can be explained physically. *Li et al.* [2010] found that the storm intensity is dependent on the solar wind reconnection electric field, E_{K-L} [*Kan and Lee, 1979*], which represents the reconnection rate between IMF and dayside magnetic field of the magnetosphere. Most of the energy that enters into the magnetosphere from the solar wind is due to the dayside reconnection mechanism. A higher reconnection rate during the main phase will result in higher energy input into the magnetosphere during that time period, which then causes a magnetic storm with a larger magnitude. On the other hand, a more intense storm would usually take a longer time for recovery, which would also lead to higher energy input during the recovery phase. This explains why there is more total energy transports into the magnetosphere during the total storm period for a more intense storm.

[19] For comparison, we listed the results of the total energy inputs with different models of l_0 in Table 2. The energy ranges with the model of $l_0 = r_0$ are quite similar to those with the model of $l_0 = 7R_E$, and the total energy inputs with the model of $l_0 = L_{CF}$ are much less, about one third of the values of the other two models. However, the high linear correlations between the total energy input and the storm intensity remain for all three models as expected. Because of the highest linear correlations between the total energy input and the storm intensity, $l_0 = 7R_E$ is used in the following estimation on the total energy input.

[20] Table 3 shows the mean values of storm-time solar wind kinetic energy (E_{SW}), total energy input (E_M), and energy input efficiency (IE) during different storm stages for three storm groups with different intensity. Energies are expressed in 10^{16} J. The values in the bracket are for the main phase, the recovery phase and the entire storm, respectively. Similar to the total energy input (E_M), solar wind kinetic energy (E_{SW}) and the input efficiency (IE) are also positively correlated to the storm intensity. For the moderate storms ($-100 < SYMH \leq -50$ nT), the mean input efficiencies during the main phase, the recovery phase and the total storm period, are 4.5%, 1.9%, and 2.8%, respectively. While for the superstorms ($SYMH \leq -300$ nT), the mean input efficiencies increase accordingly to 33.8%, 8.3% and 14.7%, respectively. The relationship between the input

Table 2. The Range of Total Energy Input (ER) for the Durations of the Main Phase, the Recovery Phase and the Total Storm Period With Different Models of l_0 , Together With the Correlation Coefficients (CC) Between the Total Energy Input and the Storm Intensity

	Main Phase	Recovery Phase	Entire Storm	Model
ER (10^{16} J)	0.32–60.73	0.05–30.19	0.98–79.86	$l_0 = 7R_E$
ER (10^{16} J)	0.14–20.82	0.03–12.10	0.47–27.11	$l_0 = L_{CF}$
ER (10^{16} J)	0.53–56.72	0.13–35.76	1.82–77.00	$l_0 = r_0$
CC	0.85	0.76	0.90	$l_0 = 7R_E$
CC	0.76	0.69	0.85	$l_0 = L_{CF}$
CC	0.78	0.60	0.73	$l_0 = r_0$

Table 3. Mean Values of Storm-Time Solar Wind Kinetic Energy (E_{SW}), Total Energy Input (E_M), and Energy Input Efficiency (IE) During Different Storm Stages for Three Storm Groups With Different Intensity^a

	Moderate Storm	Intense Storm	Superstorm
E_{SW}	(72.83, 91.71, 168.15)	(95.68, 130.81, 233.97)	(126.28, 235.84, 417.60)
E_M	(2.63, 1.54, 4.25)	(7.74, 4.48, 12.62)	(39.81, 18.54, 58.44)
IE (%)	(4.5, 1.9, 2.8)	(11.8, 4.3, 6.2)	(33.8, 8.3, 14.7)

^aEnergies are expressed in 10^{16} J. The values in the bracket are for the main phase, the recovery phase, and the entire storm, respectively.

efficiency (IE) and the storm intensity is shown in Figure 2. For the durations of the main phase, the recovery phase, and the total storm period, the input efficiencies (IE) all tend to be positively correlated to the storm intensity, with the linear correlation coefficients of 0.70, 0.45 and 0.63, respectively. Because a larger reconnection rate exists during the main phase, the input efficiency (IE) during the main phase is also larger than that during the recovery phase in general.

3.2. Partition of the Energy Dissipation

[21] The total dissipated energy in the inner M-I coupling system via ring current injection, joule heating, and auroral particle precipitation are denoted by E_{RC} , E_J , and E_A , respectively. They are calculated by integrating over time too. Note that the parameters E_J and E_A cover both the north and south hemisphere. $E_{IO} = E_J + E_A$, is the total energy dissipated via high-latitude ionosphere. A parameter, $\xi = E_{RC}/E_{IO}$, was used to describe the partition of the energy dissipation via the ring current injection and high-latitude ionospheric dissipation.

[22] Because of the critical role of ring current decay time in estimating the dissipated energy via ring current injection, to choose a proper ring current decay rate model is principal in the study of dissipated energy partition. The principal feature of a magnetic storm is a global sudden decrease of the horizontal magnetic field and its recovery. This decrease of horizontal field is known to be due to an enhancement of the ring current particle population. Hence, it is expected that the total dissipated energy via ring current injection varies directly with the storm intensity. Table 4 shows the correlation coefficients between the total dissipated energy

via ring current injection (E_{RC}) and the storm intensity by using different models of ring current decay time (τ). The linear correlations are all very good, with the coefficients more than 0.8, by using all the six models listed in Table 1. Note that, the correlation coefficient of 0.92 by using G1993 model is the highest. Therefore, G1993 model of the ring current decay rate is chosen to make the following estimations.

[23] Table 5 gives the mean values of storm-time ring current injection (E_{RC}), auroral precipitation (E_A), joule heating (E_J) and their percentages of the total energy output during different storm stages for three storm groups with different intensity. Energies are expressed in 10^{16} J. The values in the bracket are for the main phase, the recovery phase and the entire storm, respectively. E_{RC} , E_A , and E_J during different storm stages all increase as the storm intensity increases. E_{RC} during the total storm period is about 1.44×10^{16} J for the moderate storms, and it increases to 26.53×10^{16} J for the superstorms, about 18 times. E_A and E_J during the total storm period increase from 1.22×10^{16} J and 2.42×10^{16} J to 2.17×10^{16} J and 4.47×10^{16} J, respectively, about 1.8 times. For the moderate storms, the high-latitude ionospheric dissipation accounts for the vast majority of the energy dissipation, with about 71.0% of the total energy output. While for the superstorms, the ring current injection is the dominant dissipation channel, with about 78.1% of the total energy output.

[24] The correlation between the partition of the energy dissipation via the ring current injection and high-latitude ionospheric dissipation (ξ) and the storm intensity is also

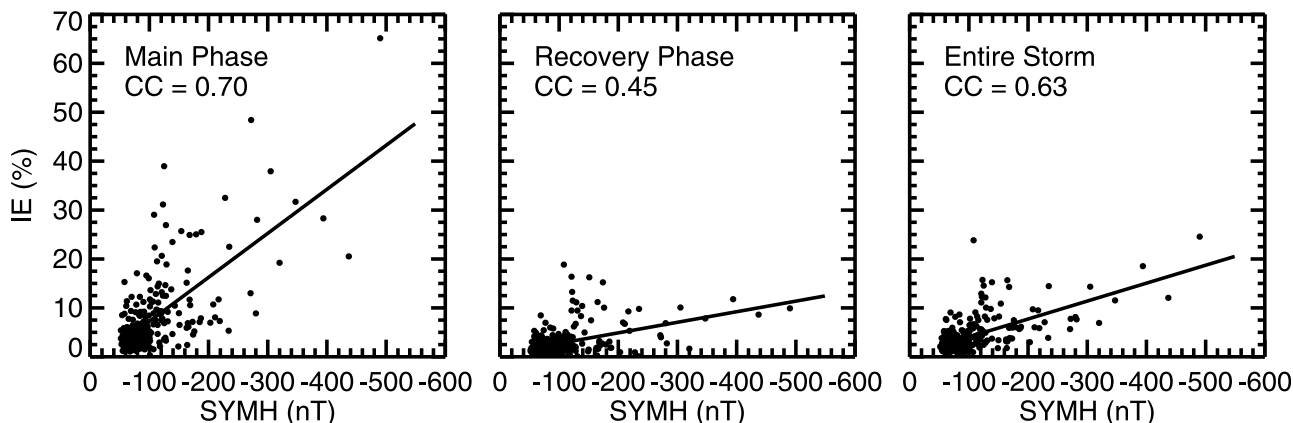


Figure 2. The relationship between the energy input efficiency (IE) and the storm intensity. The results for the durations of the main phase, the recovery phase and the total storm period are shown successively from left to right. CC is the correlation coefficient.

Table 4. Correlation Coefficients (CC) Between the Total Dissipated Energy via Ring Current Injection (E_{RC}) During the Total Storm Period and the Storm Intensity by Using Different Models of Ring Current Decay Time (τ).

CC	Model
0.82	BM1975
0.91	A1981
0.92	G1993
0.83	VS1996
0.87	OM2000
0.88	XD2010

studied and shown in Figure 3. As mentioned before, we chose G1993 to be the model of the ring current decay rate in calculating the ring current injection. Our analysis clearly show that the energy dissipation via the ring current becomes more and more dominant as the storm intensity increases. The contribution of the ring current injection to the total energy dissipation is directly proportional to the storm intensity. The linear correlation coefficients for the main phase, the recovery phase and the total storm period are as high as 0.92, 0.85 and 0.90, respectively.

[25] To test the sensitivity of our results to ring current decay rate models, we also calculate the ring current injection by using different models of the ring current decay rate listed in Table 1. The correlation coefficients between ξ and the storm intensity for all the six models are listed in Table 6. The correlation coefficients for the main phase are all larger than 0.66, representing a good linear correlation between ξ and the storm intensity. These results further confirm that the partition of energy dissipation in the inner M-I coupling system does dependent on the storm intensity, which would help to further understand the energy partition between magnetic storms and substorms.

3.3. Energy Budget

[26] Another important issue of the storm-time magnetospheric energetics is the energy budget. An energy coupling efficiency (CE) was used by *Turner et al.* [2009] to represent the energy budget. The expression of CE is shown as follows:

$$CE = \frac{\text{energy dissipation}}{\text{energy input}} = \frac{E_{RC} + E_{IO}}{E_M} \times 100\% \quad (8)$$

When CE is less than 100%, residual energy would be stored in the magnetosphere; when CE is greater than 100%, there needs additional energy source to supply the energy sinks in the inner M-I coupling system during the magnetic storms.

[27] Figure 4 shows the relationship between the coupling efficiency (CE) and the storm intensity. As the storm intensity increases, CE seems to decay exponentially, especially during the main phase and the total storm period. The solid line represents the exponential fitting. R^2 represents the fitting efficiency, and 1 represents a perfect fitting. On the whole, CE during the main phase is less than that during the recovery phase. For the intense storms with $SYM_H \leq -200$ nT, CE is less than 60% and decreases gradually as the storm intensity increases. While for some moderate storms, CE is even larger than 100%, especially in the duration of the recovery phase.

[28] Table 7 gives the mean values of storm-time magnetospheric energy budget and energy coupling efficiency (CE) during different storm stages for three storm groups with different intensity. Similar to Tables 3 and 5, energies are expressed in 10^{16} J, and the values in the bracket are for the main phase, the recovery phase and the entire storm, respectively. For the intense and super storms, CE during the total storm period is less than 100%, which may suggest that the energy entered into the magnetosphere from the solar wind is not always released fully during an intense storm, and some of which can be stored in the magnetosphere and serves as an additional energy source to supply the later moderate storms. While for the moderate storms, CE during the total storm period is larger than 100%, which may suggest that the energy dissipation in the inner M-I coupling system for some moderate storms is not only at the expense of energy that is directly transported into the magnetosphere from the solar wind, but rather at the expense of energy previously stored in the magnetosphere.

4. Discussion

[29] To study the storm-time magnetospheric energetics, it is first particularly important to determine how much energy is transferred into the magnetosphere from the solar wind during storm events and its efficiency. Although the model of $l_0 = 7R_E$ we used in estimating the energy input seems to be physical meaningless, it leads to the best linear correlation between the total energy input and the storm intensity as we expected. *Gonzalez et al.* [1989] investigated ten intense storms, finding that the mean efficiency of the energy transferred from the solar wind into the magnetosphere is about 10%. *Mac-Mahon and Gonzalez* [1997] used $l_0 = L_{CF}$ model and studied four extreme intense magnetic storms (the mean *Dst* index was ~ -290 nT), finding that about 1% and 4% of the solar wind kinetic energy is transferred into the magnetosphere. Similar results were also obtained by *Vichare et al.* [2005] (3.2%) and *Lu et al.* [1998] (4.2%). Our result shows that the input efficiency increases with the storm intensity, from $\sim 2.8\%$ for the moderate storms to $\sim 14.7\%$ for the superstorms. The mean value for all the storms is 4.0%. The variation range is consistent with the previous studies.

[30] With a determination of energy input, it is then of further great value to study quantitatively how the input energy is partitioned among the several energy dissipation “branches”. *Perreault and Akasofu* [1978] argued that

Table 5. Mean Values of Storm-Time Ring Current Injection (E_{RC}), Auroral Precipitation (E_A), Joule Heating (E_J) and Their Percentages of the Total Energy Output During Different Storm Stages for Three Storm Groups With Different Intensity^a

	Moderate Storm	Intense Storm	Superstorm
E_{RC}	(0.70, 0.71, 1.44)	(1.84, 2.56, 4.47)	(7.95, 16.77, 26.53)
Percentage (%)	(28.9, 29.4, 29.0)	(46.2, 46.8, 45.8)	(80.8, 77.5, 78.1)
E_A	(0.58, 0.63, 1.22)	(0.64, 0.89, 1.56)	(0.55, 1.54, 2.17)
Percentage (%)	(22.8, 25.0, 24.0)	(16.5, 18.4, 17.7)	(6.0, 7.8, 7.1)
E_J	(1.25, 1.14, 2.42)	(1.47, 1.72, 3.26)	(1.21, 2.88, 4.47)
Percentage (%)	(48.3, 45.6, 47.0)	(37.3, 34.8, 36.5)	(13.1, 14.7, 14.8)

^aEnergies are expressed in 10^{16} J. The values in the bracket are for the main phase, the recovery phase, and the entire storm, respectively.

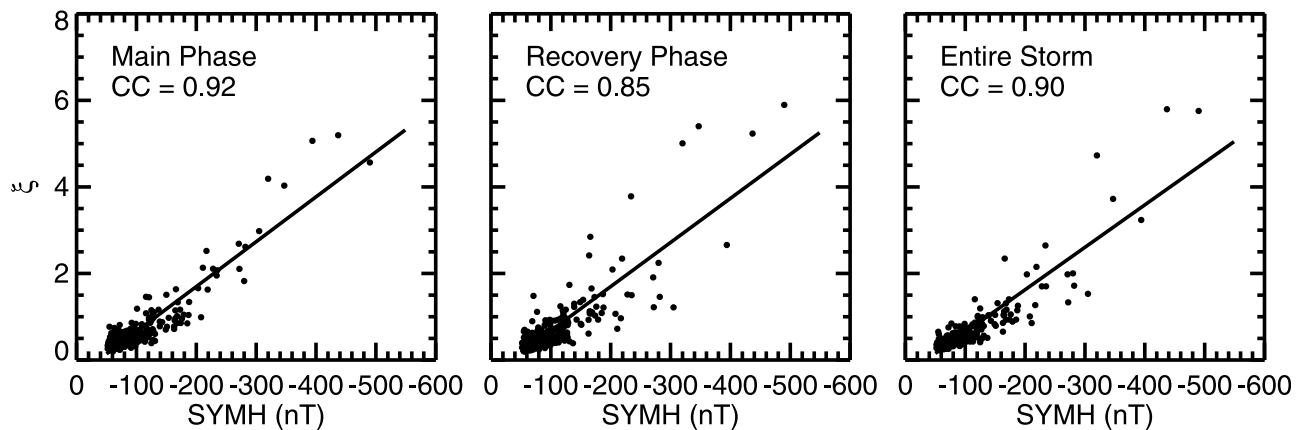


Figure 3. The dependent of the dissipated energy partition via the ring current and high-latitude ionosphere on the storm intensity. The results for the durations of the main phase, the recovery phase and the total storm period are shown successively from left to right. CC is the correlation coefficient.

~90% of energy dissipation would be through ring current injection. *Mac-Mahon and Gonzalez* [1997] studied four extreme intense magnetic storms (the mean Dst index was ~ -290 nT) and found that the energy dissipation via the high-latitude ionosphere was about half of the ring current injection. Their result was later supported by *Vichare et al.* [2005]. By analyzing nine intense magnetic storms (the mean Dst index was ~ -255 nT), *Vichare et al.* [2005] found that the contribution of ring current injection in the energy dissipation was $\sim 60\%$. On the other hand, many recent studies based on case analysis gave much less values. *Lu et al.* [1998] found that the contribution of the ring current was only $\sim 30\%$ in a moderate magnetic storm (one storm event, $Dst = -85$ nT) by using the assimilation mapping of ionospheric electrodynamics (AMIE) method. Similar results were also obtained by *Knipp et al.* [1998] (one storm event, $Dst = -116$ nT), *Baker et al.* [2001] (one storm event, $Dst = -85$ nT) and *Feldstein et al.* [2003] (two storm events, the mean Dst index was ~ -152 nT). Actually, their results were not in disagreement because one is for intense storms, the other is for moderate storms. Our analyses of 307 magnetic storms enable us to see how the partition of energy dissipation in the inner M-I coupling system actually dependent on the storm intensity. For moderate storms, the high-latitude ionospheric dissipation accounts for the vast majority of the energy dissipation, with about 71.0% of the total energy output, which is consistent with the results of *Lu et al.* [1998], *Knipp et al.* [1998], *Baker et al.* [2001], and *Feldstein et al.* [2003]. While for superstorms, the ring current injection is the dominant dissipation channel, with about 78.1% of the total energy output, which is also consistent with the results of *Mac-Mahon and Gonzalez* [1997] and *Vichare et al.* [2005]. *Turner et al.* [2009] and *Guo et al.* [2011] both made a statistical survey of the storm-time energy partition, reporting that only 10–11.5% ($Dst \leq -50$ nT) and 12–14% ($Dst \leq -100$ nT) of input energy is dissipated by ring current injection. While our results disagree with their results. The ring current injection is about 34.7% ($Dst \leq -50$ nT) and 47.8% ($Dst \leq -100$ nT) of total energy output. The great discrepancies come from the

different ring current decay time model used in our respective estimations. The magnitude of the ring current injection depends strongly on the decay time. The larger decay time is used, the less ring current injection would be estimated. *Turner et al.* [2009] and *Guo et al.* [2011] both fixed ring current decay rate (τ) to be 8 hours, while we used the G1993 model listed in Table 1 with less than 1 hour for intense magnetic storms. They would underestimate the ring current injection. *Guo et al.* [2011] also examined the influence of τ , finding the ring current injection accounts for a larger percentage with a less value of τ .

[31] At last, it is also necessary to study the energy budget during storms. *Guo et al.* [2011] reported that the mean coupling efficiency (ration of total energy output to total energy input) is $\sim 60\%$, While it is $\sim 85.7\%$ in our analysis. This is probably because *Guo et al.* [2011] underestimated the ring current injection by using a relative larger ring current decay time ($\tau = 8$ hours). Note that, some substorm-related tail energy sinks are not considered in studying the energy budget, such as escape energy carried by plasmoids and plasma sheet heating [*Baker et al.*, 1997; *Ieda et al.*, 1998; *Honkonen et al.*, 2011]. *Koskinen and Tanskanen* [2002] suggested that a scaling parameter of 1.5–2 should be applied to the coupling parameters to account for some substorm-related tail energy sinks in calculating the energy input from the solar wind to the magnetosphere. Therefore, although the tail energy sinks are not considered, the origin

Table 6. Correlation Coefficients (CC) Between the Partition of the Energy Dissipation via the Ring Current Injection and High-Latitude Ionospheric Dissipation (ξ) and the Storm Intensity by Using Different Models of Ring Current Decay Time (τ)

	Main Phase	Recovery Phase	Entire Storm	Model
CC	0.67	0.34	0.54	BM1975
CC	0.88	0.77	0.89	A1981
CC	0.92	0.85	0.90	G1993
CC	0.66	0.31	0.54	VS1996
CC	0.72	0.38	0.63	OM2000
CC	0.79	0.74	0.87	XD2010

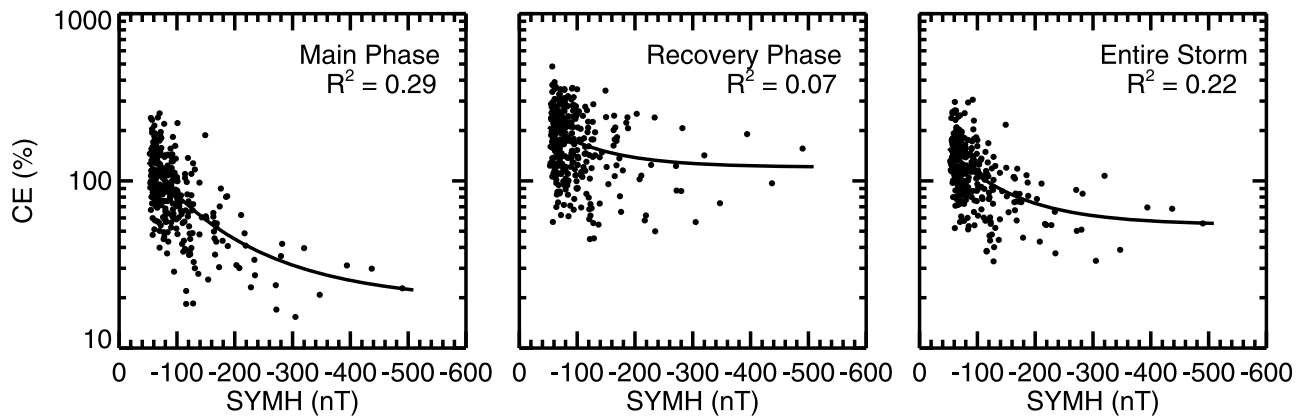


Figure 4. The relationship between the coupling efficiency (CE) and the storm intensity. The results for the durations of the main phase, the recovery phase and the total storm period are shown successively from left to right. R^2 represents the exponential fitting efficiency.

coupling parameter ($l_0 = 7R_E$) used here makes the coupling efficiency still reasonable.

5. Concluding Remarks

[32] Our statistical results from analyzing 307 magnetic storms enable us to give a relatively comprehensive depiction of storm-time magnetospheric energetics, such as the partition of energy dissipation, the energy input from the solar wind into the magnetosphere and its efficiency, and the energy budget. Furthermore, the energetics involved in the storm main phase, the recovery phase and the total storm period are studied separately to gain a detailed understanding of the energy processes. The main results are remarked as follows.

[33] 1. The partition of the energy dissipation via the ring current injection and the high-latitude ionospheric dissipation is controlled by the storm intensity. The proportions of the ring current injection during the main phase, the recovery phase and the total storm period all increase linearly as the storm intensity increases. For moderate storms, the high-latitude ionospheric dissipation is dominant, with only $\sim 30\%$ energy dissipated via the ring current; whereas for the superstorms, the ring current injection becomes dominant, with $\sim 70\%$ energy dissipated via the ring current. This phenomenon would help to further understand the energy partition between magnetic storms and substorms.

[34] 2. It is confirmed that the essential and crucial role of the total energy input into the magnetosphere during the main phase in controlling the storm intensity. Their correlate

coefficient is as high as 0.85. For the durations of the main phase, the recovery phase, and the total storm period, the input efficiencies all tend to be positively correlated to the storm intensity, with the linear correlation coefficients of 0.70, 0.45 and 0.63, respectively. Moreover, the input efficiency during the main phase is larger than that during the recovery phase.

[35] 3. The energy budget during magnetic storms is quantified. The coupling efficiency seems to decay exponentially as the storm intensity increases. For the intense storms, CE is less than 60% and decreases gradually as the storm intensity increases, whereas for some moderate storms, CE is much greater, even larger than 100%. This phenomenon may suggest that the energy entered into the magnetosphere is not always released fully during an intense storm, some of which can be stored in the magnetosphere and serves as an additional energy source for the later moderate storms. Although the tail energy sinks are not considered, the origin coupling parameter ($l_0 = 7R_E$) used here makes the coupling efficiency still reasonable. Global MHD simulation can be a good approach to estimate the magnetotail energy sinks in the future. With all magnetotail energy sinks considered, the study of energy budget would be more accurate.

[36] **Acknowledgments.** We acknowledge the use of OMNI-5min data from <ftp://cdaweb.gsfc.nasa.gov/pub/istp/omni>. We also thank the Kyoto World Data Center for providing the AE/SYMH indices. This work was supported by 973 program 2012CB825602, NNSFC grants 40921063 and 40831060, and in part by the Specialized Research Fund for State Key Laboratories of China. H. Li was also supported by the Open Research Program of Key Laboratory of Geospace Environment, Chinese Academy of Sciences.

Table 7. Mean Values of Storm-Time Magnetospheric Energy Budget and Energy Coupling Efficiency (CE) During Different Storm Stages for Three Storm Groups With Different Intensity^a

	Moderate Storm	Intense Storm	Superstorm
Total energy input	(2.63, 1.54, 4.25)	(7.74, 4.48, 12.62)	(39.81, 18.54, 58.44)
Total energy output	(2.53, 2.48, 5.09)	(3.95, 5.17, 9.28)	(9.71, 21.19, 33.17)
CE (%)	(105.6, 210.5, 132.8)	(62.2, 220.3, 87.3)	(25.3, 169.2, 62.0)

^aEnergies are expressed in 10^{16} J. The values in the bracket are for the main phase, the recovery phase, and the entire storm, respectively.

References

- Ahn, B. H., S.-I. Akasofu, and Y. Kamide (1983), The Joule heat production rate and the particle energy injection rate as a function of the geomagnetic indices AE and AL, *J. Geophys. Res.*, *88*, 6275–6287.
- Ahn, B. H., H. W. Kroehl, Y. Kamide, and D. J. Gorney (1989), Estimation of ionospheric electrodynamic parameters using ionospheric conductance deduced from Bremsstrahlung X-ray image data, *J. Geophys. Res.*, *94*, 2565–2586.
- Akasofu, S.-I. (1981), Energy coupling between the solar wind and the magnetosphere, *Space Sci. Rev.*, *28*, 121–190.
- Baker, D. N., T. I. Pulkkinen, M. Hesse, and R. L. McPherron (1997), A quantitative assessment of energy storage and release in the Earth's magnetotail, *J. Geophys. Res.*, *102*, 7159–7168.
- Baker, D. N., N. E. Turner, and T. I. Pulkkinen (2001), Energy transport and dissipation in the magnetosphere during geomagnetic storms, *J. Atmos. Sol. Terr. Phys.*, *63*, 421–429.
- Baumjohann, W., and Y. Kamide (1984), Hemispherical Joule heating and the AE indices, *J. Geophys. Res.*, *89*, 383–388.
- Burton, R. K., R. L. McPherron, and C. T. Russell (1975), An empirical relationship between interplanetary conditions and Dst, *J. Geophys. Res.*, *80*, 4204–4214.
- Cooper, M. L., C. R. Clauer, B. A. Emery, A. D. Richmond, and J. D. Winningham (1995), A storm time assimilative mapping of ionospheric electrodynamic analysis for the severe geomagnetic storm of November 8–9, 1991, *J. Geophys. Res.*, *100*, 19,329–19,342.
- Dungey, J. W. (1961), Interplanetary magnetic field and the auroral zones, *Phys. Rev. Lett.*, *6*, 47–48.
- Feldstein, Y. I. (1992), Modeling of the magnetic field of magnetospheric ring current as a function of interplanetary medium parameters, *Space Sci. Rev.*, *59*(1–2), 83–165.
- Feldstein, Y. I., L. A. Dremukhina, A. E. Levitin, U. Mall, I. I. Alexeev, and V. V. Kalegaev (2003), Energetics of the magnetosphere during the magnetic storm, *J. Atmos. Sol. Terr. Phys.*, *65*, 429–446.
- Gonzalez, W. D. (1993), Ring current evolution during intense magnetic storms, paper presented at Magnetic Storm/Substorm Relationship Workshop, Natl. Geophys. Data Cent., Breckenridge, Colo., 24–27 June.
- Gonzalez, W. D., B. T. Tsurutani, A. L. C. Gonzalez, E. J. Smith, F. Tang, and S.-I. Akasofu (1989), Solar wind-magnetosphere coupling during intense magnetic storms, *J. Geophys. Res.*, *94*, 8835–8851.
- Gonzalez, W. D., J. A. Joselyn, Y. Kamide, H. W. Kroehl, G. Rostoker, B. T. Tsurutani, and V. M. Vasyliunas (1994), What is a geomagnetic storm?, *J. Geophys. Res.*, *99*, 5771–5792.
- Guo, J., X. Feng, B. A. Emery, J. Zhang, C. Xiang, F. Shen, and W. Song (2011), Energy transfer during intense geomagnetic storms driven by interplanetary coronal mass ejections and their sheath regions, *J. Geophys. Res.*, *116*, A05106, doi:10.1029/2011JA016490.
- Honkonen, I., M. Palmroth, T. I. Pulkkinen, P. Janhunen, and A. Aikio (2011), On large plasmoid formation in a global magnetohydrodynamic simulation, *Ann. Geophys.*, *29*, 167–179, doi:10.5194/angeo-29-167-2011.
- Ieda, A., S. Machida, T. Mukai, Y. Saito, T. Yamamoto, A. Nishida, T. Terasawa, and S. Kokubun (1998), Statistical analysis of the plasmoid evolution with Geotail observations, *J. Geophys. Res.*, *103*, 4453–4465, doi:10.1029/97JA03240.
- Kan, J. R., and L. C. Lee (1979), Energy coupling function and solar wind-magnetosphere dynamo, *Geophys. Res. Lett.*, *6*, 577–580.
- Knipp, D. J., et al. (1998), An overview of the early November 1993 geomagnetic storm, *J. Geophys. Res.*, *103*, 26,197–26,220.
- Knipp, D. J., W. K. Tobiska, and B. A. Emery (2004), Direct and indirect thermospheric heating sources for solar cycles 21C23, *Sol. Phys.*, *224*, 495C505, doi:10.1007/s11207-005-6393-4.
- Koskinen, H. E. J., and E. Tanskanen (2002), Magnetospheric energy budget and the epsilon parameter, *J. Geophys. Res.*, *107*(A11), 1415, doi:10.1029/2002JA009283.
- Li, H., C. Wang, and J. R. Kan (2010), Midday magnetopause shifts earthward of geosynchronous orbit during geomagnetic superstorms with Dst \leq -300 nT, *J. Geophys. Res.*, *115*, A08230, doi:10.1029/2009JA014612.
- Liou, K., P. T. Newell, C.-I. Meng, M. Brittnacher, and G. Parks (1998), Characteristics of the solar wind controlled auroral emissions, *J. Geophys. Res.*, *103*, 17,543–17,557, doi:10.1029/98JA01388.
- Lu, G., D. Richmond, B. A. Emery, and R. G. Roble (1995), Magnetosphere-ionosphere-thermosphere coupling: effect of neutral winds on energy transfer and field-aligned current, *J. Geophys. Res.*, *100*, 19,643–19,659.
- Lu, G., et al. (1998), Global energy deposition during the January 1997 magnetic cloud event, *J. Geophys. Res.*, *103*, 11,685–11,694.
- Mac-Mahon, R. M., and W. D. Gonzalez (1997), Energetics during the main phase of geomagnetic superstorms, *J. Geophys. Res.*, *102*, 14,199–14,207.
- Maltsev, Y. P. (2004), Points of controversy in the study of magnetic storms, *Space Sci. Rev.*, *110*(3–4), 227–267.
- Newell, P. T., T. Sotirelis, K. Liou, C.-I. Meng, and F. J. Rich (2007), A nearly universal solar wind-magnetosphere coupling function inferred from 10 magnetospheric state variables, *J. Geophys. Res.*, *112*, A01206, doi:10.1029/2006JA012015.
- Nishida, A. (1983), IMF control of the Earth's magnetosphere, *Space Sci. Rev.*, *34*, 185–200.
- O'Brien, T. P., and R. L. McPherron (2000), An empirical phase space analysis of ring current dynamics: solar wind control of injection and decay, *J. Geophys. Res.*, *105*, 7707–7719.
- Østgaard, N., G. Germany, J. Stadsnes, and R. R. Vondrak (2002a), Energy analysis of substorms based on remote sensing tech solar wind measurements, and geomagnetic indices, *J. Geophys. Res.*, *107*(A9), 1233, doi:10.1029/2001JA002002.
- Østgaard, N., R. R. Vondrak, J. W. Gjerloev, and G. A. Germany (2002b), A relation between the energy deposition by electron precipitation and geomagnetic indices during substorms, *J. Geophys. Res.*, *107*(A9), 1246, doi:10.1029/2001JA002003.
- Perreault, P., and S. I. Akasofu (1978), A study of geomagnetic storms, *Geophys. J. R. Astron. Soc.*, *54*, 547–573.
- Prigancova, A., and Y. I. Feldstein (1992), Magnetospheric storm dynamics in terms of energy output rate, *Planet. Space Sci.*, *40*, 581–588.
- Richmond, A. D., et al. (1990), Global measures of ionospheric electrodynamic activity inferred from combined incoherent scatter radar and ground magnetometer observations, *J. Geophys. Res.*, *95*, 1061–1071.
- Rosenqvist, L., S. Buchert, H. Opgenoorth, A. Vaivads, and G. Lu (2006), Magnetospheric energy budget during huge geomagnetic activity using Cluster and ground-based data, *J. Geophys. Res.*, *111*, A10211, doi:10.1029/2006JA011608.
- Shue, J.-H., et al. (1998), Magnetopause location under extreme solar wind conditions, *J. Geophys. Res.*, *103*, 17,691–17,700.
- Sibeck, N., R. E. Lopez, and E. C. Roelof (1991), Solar wind control of the magnetopause shape, location and motion, *J. Geophys. Res.*, *96*, 5489–5495.
- Tsurutani, B. T., and W. D. Gonzalez (1997), The Interplanetary causes of magnetic storms: A review, in *Magnetic Storms*, *Geophys. Monogr. Ser.*, vol. 98, edited by B. T. Tsurutani et al., pp. 77–89, AGU, Washington, D. C.
- Turner, N. E. (2000), Solar wind-magnetosphere coupling and global energy budgets in the Earth's magnetosphere, PhD thesis, 121 pp., Univ. of Colo. at Boulder, Boulder.
- Turner, N. E., D. N. Baker, T. I. Pulkkinen, J. L. Roeder, J. F. Fennell, and V. K. Jordanova (2001), Energy content in the storm time ring current, *J. Geophys. Res.*, *106*, 19,149–19,156.
- Turner, N. E., W. D. Cramer, S. K. Earles, and B. A. Emery (2009), Geoefficiency and energy partitioning in CIR-driven and CME-driven storms, *J. Atmos. Sol. Terr. Phys.*, *71*, 1023–1031.
- Valdivia, J. A., A. S. Sharma, and K. Papadopoulos (1996), Prediction of magnetic storms by nonlinear models, *Geophys. Res. Lett.*, *23*, 2899–2902.
- Vichare, G., S. Alex, and G. S. Lakhina (2005), Some characteristics of intense geomagnetic storms and their energy budget, *J. Geophys. Res.*, *110*, A03204, doi:10.1029/2004JA010418.
- Weiss, L. A., P. H. Reiff, J. J. Moses, R. A. Heelis, and D. B. Moore (1992), Energy dissipation in substorms, in *Substorms 1*, *ESA SP-335*, pp. 309–317, Eur. Space Agency, Paris.
- Xu, W. Y., and A. M. Du (2010), Effect of the ring current decay rate on the energy state of the magnetosphere, *Chin. J. Geophys.*, *53*(3), 329–338.
- Zwickl, R. D., L. F. Bargatze, D. N. Baker, C. R. Clauer, and R. L. McPherron (1987), An evaluation of the total magnetospheric energy output parameter, in *Magnetotail Physics*, edited by A. T. Y. Lui, pp. 155–159, Johns Hopkins Univ. Press, Baltimore, Md.